MR Evaluation of Chiari I Malformations at 0.15 T

Efstathios Spinos, D. Wayne Laster, Dixon M. Moody, Marshall R. Ball, Richard L. Witcofski and David L. Kelly, Jr.

AJNR Am J Neuroradiol 1985, 6 (2) 203-208
http://www.ajnr.org/content/6/2/203

MR Evaluation of Chiari I Malformations at 0.15 T

Efstathios Spinos[1]
D. Wayne Laster[1]
Dixon M. Moody[1]
Marshall R. Ball[1]
Richard L. Witcofski[1]
David L. Kelly, Jr.[2]

Twelve patients with known or presumed Chiari I malformations and two with clinical diagnoses of multiple sclerosis were examined by magnetic resonance (MR) imaging. MR confirmed or established the diagnosis of Chiari I malformation in all 14 cases. The spin-echo technique with a short time to echo (TE = 40 msec) and a short time to recover (TR = 1000 msec) provided optimum imaging of tonsillar position, hydromyelia cavities, and cervicomedullary "kinking." Long TE (>80 msec) and TR (>2000 msec) increase the signal intensity of cerebrospinal fluid and may obscure the pathology. Sagittal, transaxial, and coronal images provided complementary data; sagittal and coronal views best imaged the abnormal spinal cord and tonsils, but slitlike cavities were best seen on transaxial images. Cervicomedullary kinking was found in 10 (71%) of 14 patients and in 90% of the hydromyelic patients. This high incidence suggests that in other radiologic techniques tonsillar herniation masks the kinking. Symptoms of the Chiari I malformation overlap those of demyelinating diseases and brain tumors. Our early experience suggests MR is the preferred noninvasive procedure for identifying Chiari I malformation. Moreover, the ability to portray the variable cavity morphology of hydromyelia directly offers the potential for improved shunt placement.

The Chiari I malformation, a hindbrain dysgenesis, results in abnormal cerebellar tonsil morphology and position. Hydromyelia occurs in 50% of the cases and arachnoid adhesions are a common operative finding. In contrast to Chiari II malformation, the position of the fourth ventricle is normal. "Kinking," backward and downward displacement of the cervicomedullary junction, has been documented, but its incidence is reported as 12% [1].

Two conventional neuroradiologic methods combining vertebral angiography, pneumoencephalography, or myelography are generally required for Chiari I diagnosis [2, 3]. All of these procedures are uncomfortable, time-consuming, and potentially dangerous.

Computed tomography (CT), a noninvasive imaging technique, provides inadequate delineation of tissue below the foramen magnum. Intrathecal injection of metrizamide before CT (metrizamide CT myelography) is necessary for the diagnosis of Chiari I malformations [2, 4–6].

The superiority of magnetic resonance (MR) imaging in the evaluation of the posterior fossa and spinal cord has been demonstrated by several authors [7–11]. Most published images and techniques were at higher field strengths. MR is not subject to bone artifacts, is capable of direct triplanar imaging of contiguous sections, and provides better tissue contrast than metrizamide CT without the risk associated with intrathecal injection, if optimum pulse sequences are used [8]. Our experience with MR at 0.15 T of both surgically proven and previously unsuspected Chiari I malformations is described. Details of our methods including optimal techniques for visualizing cerebellar tonsils, hydromyelia cavities, and Shunt tubes are presented.

This article appears in the March/April 1985 issue of *AJNR* and the June 1985 issue of *AJR*.

Received May 30, 1984; accepted after revision August 14, 1984.

E. Spinos is a neuroradiology fellow.

[1] Department of Radiology, Bowman Gray School of Medicine, Wake Forest University, 300 S. Hawthorne Rd., Winston-Salem, NC 27103. Address reprint requests to D. W. Laster.

[2] Department of Surgery, Section of Neurosurgery, Bowman Gray School of Medicine, Wake Forest University, Winston-Salem, NC 27103.

***AJNR* 6:203–208, March/April 1985**
0195–6108/85/0602–0203

Fig. 1.—Midline sagittal SE 700/40 image in normal volunteer. Note position of cerebellar tonsils at level of foramen magnum (*arrow*) and globular shape of inferior surface. Cisterna magna and other pericerebellar cisterns are clearly seen as is fourth ventricle. Junction of medulla with cervical cord is smooth with minimal angulation.

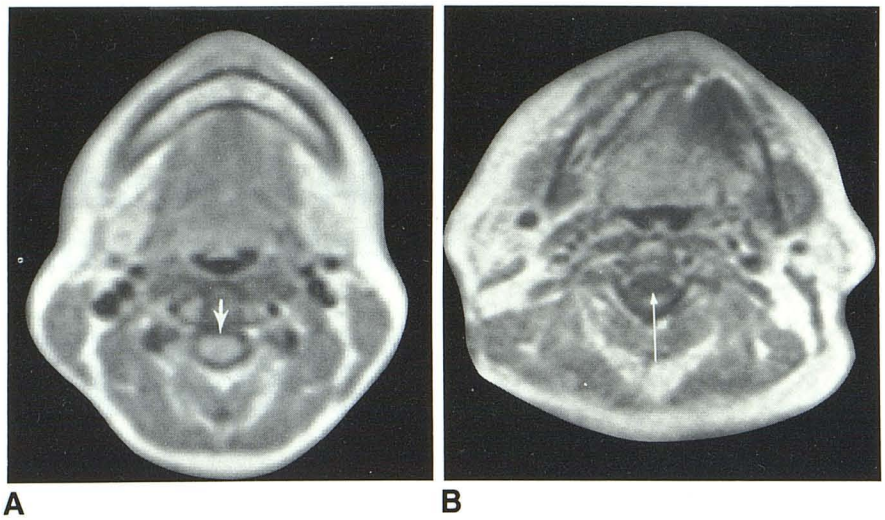

A B

Fig. 2.—Transaxial SE 700/40 images. **A**, Normal volunteer. High-intensity cervical cord surrounded by low-intensity CSF (*arrow*). **B**, Chiari patient with hydromyelia. High-intensity nervous tissue is thin rim surrounding large, low-intensity CSF-filled cavity (*arrow*).

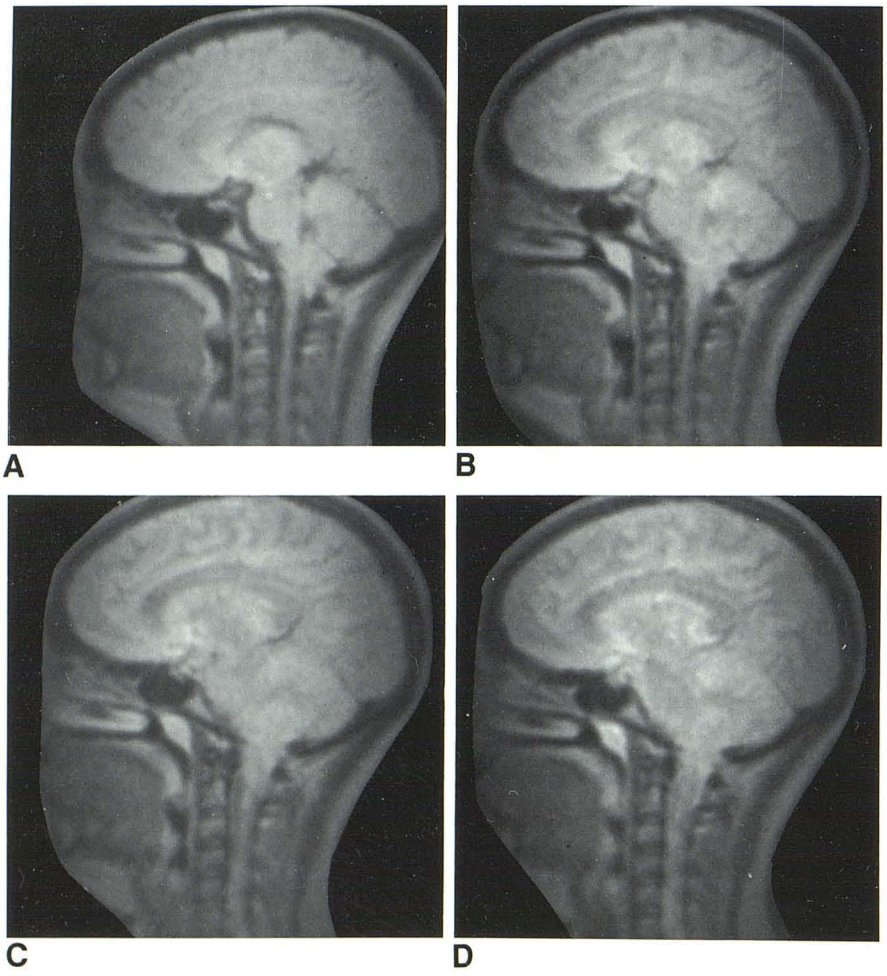

A B C D

Fig. 3.—SE 1000/40 (**A**), SE 2000/40 (**B**), SE 3000/40 (**C**), and SE 4000/40 (**C**) images of Chiari I malformation. Increasing TR from 1000 to 4000 msec diminishes distinction between cervical cord and tonsils by increasing signal from surrounding CSF.

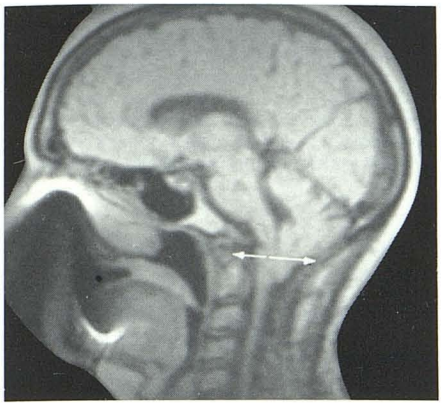

Fig. 4.—Midline sagittal SE 900/40 image in Chiari I patient. Note position of cerebellar tonsils below level of foramen magnum (*arrow*) and peglike configuration. Prominent kinking of cervicomedullary junction.

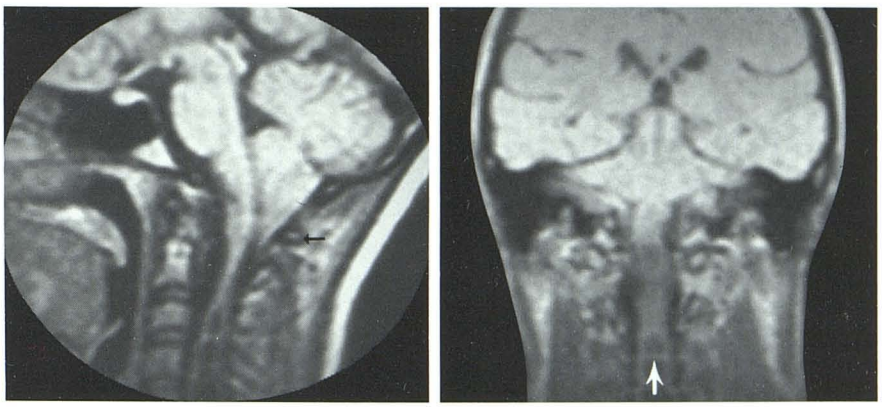

A B

Fig. 5.—SE 700/40 images in patient with Chiari I malformation and hydromyelia. **A**, Sagittal image. Peglike tonsils positioned below posterior arch of C1 (*arrow*). Kinking of cervicomedullary junction. **B**, Coronal image. Large cervical hydromyelia cavity with prominent transverse septations (*arrow*). Low signal at C1–C2 is from cord position posteriorly out of MR plane.

Subjects and Methods

Fourteen patients (five men and nine women) and several normal volunteers were studied. In 10 patients, the initial diagnosis of Chiari I malformation was made by a conventional technique such as metrizamide CT myelography, pneumoencephalography, or positive contrast myelography. The diagnosis of hydromyelia was confirmed by direct instillation of water-soluble contrast material into the cavity in two cases and by delayed metrizamide CT myelography in a third. One patient had undergone a posterior fossa decompression; another had a shunt tube in his cervical hydromyelia cavity. In three patients, MR imaging established the initial Chiari I diagnosis; two unsuspected cases had been referred with clinical diagnoses of multiple sclerosis. High-resolution MR images of a typical normal volunteer are included for anatomic comparison (fig. 1).

Patients were studied on an MR resistive-magnet prototype imager manufactured by Picker International (Picker 1000) and operating at a frequency of 6.4 MHz with a magnetic field of 0.15 T (1500 G). A 30 cm aperture was used for head and upper cervical images and a 45 cm aperture for more distal cord images. MR data were processed using a two-dimensional Fourier transform technique. Multislice acquisition of four, eight, and 16 slice sequences was used. Average slice thickness was 10 mm. Transaxial, coronal, and sagittal images were displayed on a 256 × 256 matrix. The spin-echo (SE) pulse sequence was used with a time to echo (TE = 40 msec) and a time to recover (TR) varying from 700 msec for a single slice to 4050 msec for a 16 slice acquisition.

Multiplanar Imaging

The need for imaging in multiple planes has been expressed by several authors [8, 12, 13]. Sagittal and coronal views were best for demonstrating tonsillar position and cord morphology. Six of seven known hydromyelia cavities were imaged using these planes, but small, slitlike cavities were best seen on transaxial images (fig. 2).

Contiguous Sections

Contiguous sections are necessary when imaging in coronal or sagittal planes. Curvature of the spine and the difficulty in positioning some patients resulted in inadequate images when a single-slice technique was used to image the cord. Multislice contiguous sections proved the most efficient.

Pulse Sequence Techniques

In MR imaging, contrast between cerebrospinal fluid (CSF) and brain or spinal cord varies with the TE and TR used. A short TE (40 msec) and TR (under 1000 msec) result in a low signal intensity from CSF and a high signal intensity from nervous tissue. As TE and TR are increased concomitantly (it is necessary to increase TR in multislice imaging), the CSF signal is selectively increased diminishing the contrast between CSF and spinal cord. For Chiari I evalution, the best contrast was achieved using a short TE (40 msec), the shortest TR possible, and two to four averages (fig. 3).

Results

Tonsillar Position

Tonsillar position and inferior tonsillar shape were best demonstrated on sagittal images (fig. 4); however, one case of asymmetric tonsillar herniation was identified only on coronal images. The amount of cerebellar tissue below the foramen magnum varied, and in some subjects determination of its inferior extent, was obscured by the lack of separation between spinal cord and cerebellar tissue. In each case where the inferior surface of the tonsils was identified in the sagittal view, an abnormal pointed or "peglike" appearance was seen with Chiari I. Normally, the inferior surface of the imaged cerebellar tonsil is globular (fig. 1).

The use of long TR and TE times (greater than SE 2000/80) that increase the CSF signal can be a pitfall in the diagnosis of the tonsillary herniation characteristic of Chiari I malformations. Use of these parameters can cause increased CSF signal to be mistaken for tonsillar herniation (figs. 3C and 3D).

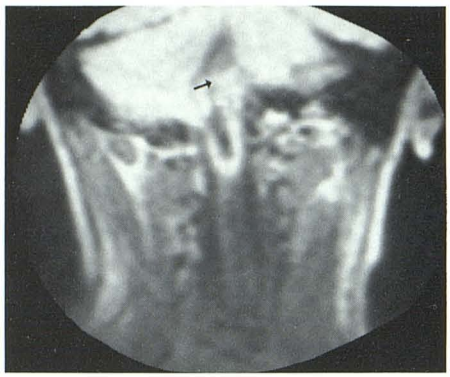

6

Fig. 6.—Coronal SE 900/40 image. Hydromyelia cavity appears to communicate with somewhat distorted fourth ventricle (*arrow*).

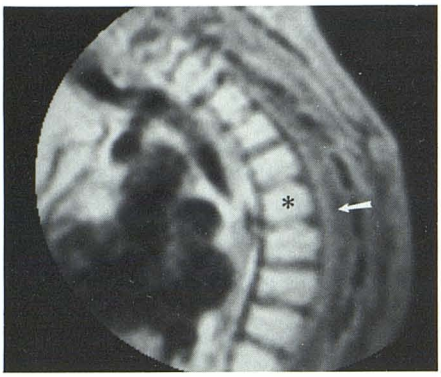

7

Fig. 7.—Midline sagittal SE 700/40 image using body coil. Large cavity (*arrow*) inferior to region of previous shunt. T7 (*).

Hydromyelia

Hydromyelia cavities were seen on MR images as areas of low signal intensity (black) in the central part of the high-signal (white) spinal cord. In three patients, transverse septations within the cavity were seen in both sagittal and coronal planes (fig. 5). Syringobulbia with the cavity extending through the medulla and joining the fourth ventricle was noted in two subjects (fig. 6).

The MR body coil was used to determine the inferior extent of spinal cord cavities. One patient who had undergone a cervical shunting procedure presented with a deteriorating clinical condition. The shunted cervical part of the cord showed no residual hydromyelia cavity indicating adequate drainage. Using the body coil, a large cavity was identified distal to the region of shunt drainage from the thoracic cord to the level of the conus (fig. 7). In another patient, metrizamide myelography demonstrated a uniformly enlarged thoracic and cervical cord. MR revealed that uniform enlargement did not correspond to the appearance of the hydromyelia cavity. Sagittal and coronal images (fig. 8) show the inner architecture of the cavity is considerably more irregular, composed of a series of fusiform expanded cavities interconnected by only moderately dilated tubular segments. The fusiform hydromyelia cavity in the conus medullaris extended into the filum terminale.

Shunt tubes, where present, were difficult to identify and were most reliably seen on transaxial images. Sagittal cord profiles of shunt recipients were irregular, suggesting cord abnormalities, but residual hydromyelia cavities were not seen. Presumably communicating cavities collapse with shunting.

Kinking

Kinking of the cervicomedullary junction occurred in 10 of the 14 Chiari I patients studied and in all of the patients with hydromelia. Sagittal images in these cases showed an anterior kinking and posterior "humping" of the cervicomedullary junction (fig. 9).

Discussion

In the most comprehensive review of the anatomic features of the Chiari I malformation, Logue and Edwards [14, 15] found craniovertebral junction anomalies, including atlantoaxial assimilation, high odontoid, short clivus, and Klippel-Feil, in 37% of cases; hydromyelia, 44%–56%; and hydrocephalus, 3%. At surgery, Paul et al. [1] found cervicomedullary kinking in 12% of patients, arachnoid adhesions in 41%, and dural bands in 30%.

MR imaging simplifies the diagnoses of Chiari I malformation and hydromyelia. Multiple planar imaging, ability to highlight different tissues through the use of various pulse sequences, freedom from bone artifacts, noninvasiveness, and lack of known biologic hazard make it the procedure of choice for intraaxial anomalies of the craniovertebral junction.

On sagittal SE images (TE 40 msec, TR $<$ 1000 msec), abnormal tonsillar position and shape, cord morphology including cervicomedullary kinking, and most hydromyelia cavities are appreciated easily. Use of the MR body coil allows the full extent of the cord to be examined for cavities so that those inferior to the cervical area will not be overlooked.

The myelographic appearance of the cord exterior does not correlate with the inner architecture of hydromyelia cavities. Although clinical improvement after syringostomy has been quite variable on long-term follow-up [16], demonstration of this inner architecture can serve to guide the neurosurgeon in shunt placement and possible shunt revision.

In this study, cervicomedullary kinking occurred in 71% of all the Chiari I patients, but in 90% of those with hydromyelia. These findings disagree with Paul et al. [1], who reported kinking in only 12% of Chiari I cases and did not consider this abnormality characteristic of the malformation. The literature is divided on this issue [16, 17]. In other surface-outlining techniques the kinking may be masked by tonsillar herniation while the sagittal tomographic architecture revealed by MR discloses the underlying kink.

A major purpose of our communication was to delineate the pulse sequence parameters best suited to diagnose the Chiari I malformation at low field strength. Contrast in MR imaging depends on proton density, relaxation times, and

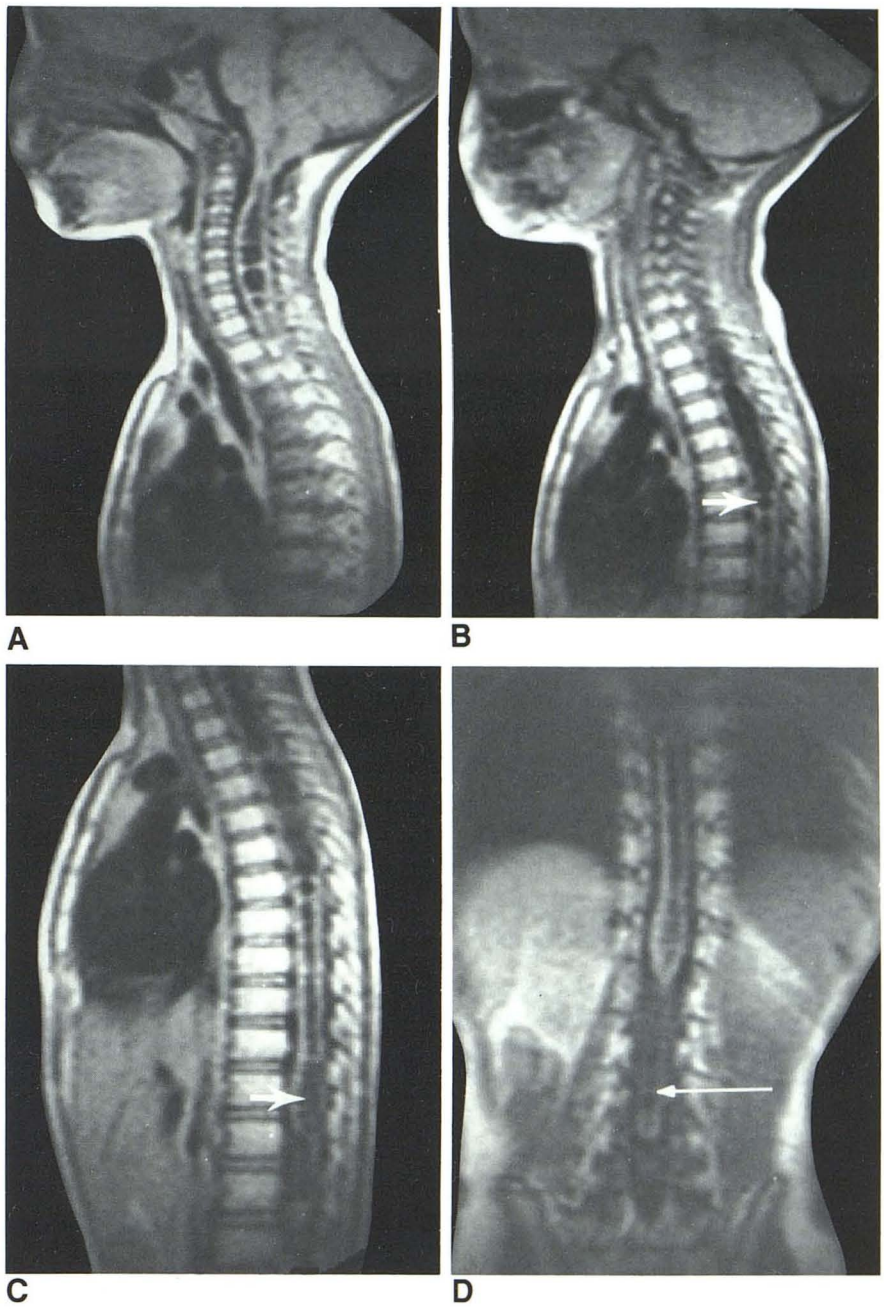

Fig. 8.—**A**, Chiari malformation with hydromyelia cavity in cervical region extending into medulla. Because of scoliosis, cord is not imaged below C7. **B**, Fusiform hydromyelia cavity in midthoracic region tapers into slightly dilated tubular segment (*arrow*). **C**, Tubular segment of cavity in **B** becomes saccular in lower thoracic region (*arrow*). **D**, Coronal plane. Extension of hydromyelia into filum terminale (*arrow*).

flow. Relative contributions of these factors are altered by manipulating the spatial resolution, object contrast, and imaging time of the technique. SE imaging with short TE and TR shows little gray/white-matter contrast but provides excellent contrast resolution between the higher signal intensity of spinal cord and the low signal intensity of the CSF. This set of parameters proved best for diagnosing Chiari I malformation, hydromyelia cavities, and cord impingement. Lengthening the TR increases gray/white-matter contrast. While this is valuable in the diagnosis of demyelinating disease, it also increases the CSF signal, thereby obscuring the Chiari I abnormalities of tonsillar herniation or hydromyelia.

The symptoms of the Chiari I malformation overlap those of demyelinating diseases and brain tumors, and accurate diagnosis is necessary for appropriate therapy. Two subjects with Chiari malformations in our study were presumed to have multiple sclerosis. MR may be the preferred noninvasive test to differentiate between these congenital, degenerative, and neoplastic disorders.

After accurate diagnosis and appropriate treatment, pa-

A B

Fig. 9.—Midline sagittal SE 900/40 images in two surgically proven cases of Chiari I malformation. Characteristic kinking of cervicomedullary junction. **A**, Patient had undergone posterior fossa decompression. **B**, Patient had undergone cervical cavity shunt.

tients with Chiari I malformation may require subsequent evaluation of surgical treatment, shunt patency, or disease progression. MR imaging provides a simple, noninvasive method for periodic follow-up of these patients.

REFERENCES

1. Paul KS, Lye RH, Strang AF, Dutton J. Arnold-Chiari malformation: review of 71 cases. *J Neurosurg* **1983**;58:183–187
2. Woosley RE, Whaley RA. Use of metrizamide in computerized tomography to diagnose the Chiari I malformation. *J Neurosurg* **1982**;56:373–376
3. DiLorenzo N, Bozzao L, Antonelli M, Fortuna A. Arnold-Chiari malformation detected by unenhanced multiplanar CT scan. *Surg Neurol* **1981**;16:340–345
4. Hochman MS, Kobetz SA, Sneider SE, Zumpano BJ. Adult Arnold-Chiari malformation type I demonstrated by CT metrizamide myelography. *Surg Neurol* **1981**;16:467–468
5. Weisberg L, Shraberg D, Meriwether RP, Robertson H, Goodman G. Computed tomographic findings in the Arnold-Chiari type I malformation. *CT* **1981**;5:1–9
6. Forbes WStC, Isherwood I. Computed tomography in syringomyelia and the associated Arnold-Chiari type I malformation. *Neuroradiology* **1978**;15:73–78
7. Modic MT, Weinstein MA, Pavlicek W, et al. Nuclear magnetic resonance imaging of the spine. *Radiology* **1983**;148:757–762
8. Yeates A, Brant-Zawadzki M, Norman D, Kaufman L, Crooks L, Newton TH. Nuclear magnetic resonance imaging of syringomyelia. *AJNR* **1983**;4:234–237
9. DeLaPaz RL, Brady TJ, Buonanno FS, et al. Nuclear magnetic resonance (NMR) imaging of Arnold-Chiari type I malformations with hydromyelia. *J Comput Assist Tomogr* **1983**;7:126–129
10. Modic MT, Weinstein MA, Pavlicek W, Boumphrey F, Starnes D, Duchesneau PM. Magnetic resonance imaging of the cervical spine: technical and clinical observations. *AJNR* **1984**;5:15–22, *AJR* **1983**;141:1129–1136
11. Bydder GM, Steiner RE, Thomas DJ, Marshall J, Gilderdale DJ, Young IR. Nuclear magnetic resonance imaging of the posterior fossa: 50 cases. *Clin Radiol* **1983**;34:173–188
12. Norman D, Mills CM, Brant-Zawadzki M, Yeates A, Crooks LE, Kaufman L. Magnetic resonance imaging of the spinal cord and canal: potentials and limitations. *AJNR* **1984**;5:9–14, *AJR* **1983**;141:1147–1152
13. Hawkes RC, Holland GN, Moore WS, Corston R, Kean DM, Worthington BS. Craniovertebral junction pathology: assessment by NMR. *AJNR* **1983**;4:232–233
14. Logue V. Fourteenth Crookshank lecture. Syringomyelia: a radiodiagnostic and radiotherapeutic saga. *Clin Radiol* **1971**;22:2–16
15. Logue V, Edwards MR. Syringomyelia and its surgical treatment—an analysis of 75 patients. *J Neurol Neurosurg Psychiatry* **1981**;44:273–284
16. Appleby A. Craniovertebral anomalies. *Proc R Soc Med* **1969**; 62:729–731
17. Welch K, Shillito J, Strand R, Fischer EG, Winston KR. Chiari I "malformation"—an acquired disorder? *J Neurosurg* **1981**; 55:604–609